Computing Predicted Errors and Uncertainty for High Resolution Photogrammetric 3D data

Amy Neuenschwander, Eric Guenther, Donald Maze-England, Thomas Bakewell, and Lori Magruder
Center for Space Research, University of Texas at Austin
3925 W Braker Lane, Austin, TX, 78759
amy@csr.utexas.edu

ABSTRACT

The utilization of high-resolution 3D point cloud data is becoming more common to a variety of DoD applications and many photogrammetric data sets are collected via small Unmanned Aircraft Systems (sUAS). Although these data are common, they do not always contain information regarding their geolocation (horizontal or vertical) uncertainties. This work addresses a critical challenge when collecting sUAS-derived point cloud data by developing a methodology to predict per-point geolocation uncertainties without the need for extensive validation. This point is particularly relevant when considering data collections for operations when collection and analysis time needs to be minimized. To accomplish this task, a full error budget accounting for a sUAS flight was conducted. This included calculating the DGPS errors and uncertainties on the ground control points and determination of structural errors produced in the 3D reconstruction software. Specifically, this work compared geopositional errors between using pseudorange code GPS (i.e., relying solely on the sUAS GPS) vs differential GPS (DGPS), as well as developed a model of structural errors produced in the Structure from Motion software. Here, the impact of utilizing ground control points during the 3D reconstruction process was tested against data when ground control was not used. It was found that the utilization of DGPS surveyed ground control points during the 3D reconstruction process reduces both relative and absolute errors of the 3D data by more than an order of magnitude. Next, two machine learning models were developed to estimate the per-point measurement errors caused by poor 3D reconstruction from the Structure from Motion software that approximates the true measured error. The result is a methodology to compute a comprehensive per-point error product for sUAS data which in a simulation or training environment adds an increased level of realism for the training mission.

ABOUT THE AUTHORS

Amy Neuenschwander is a Senior Research Scientist at the University of Texas at Austin Center for Space Research. She is a past NASA Fellow, and has over 30 years of experience in EO/IR imagery, signal processing and LiDAR analysis. Dr. Neuenschwander holds a B.S. and a Master's degree in Aerospace Engineering, and a doctorate degree in Geography and the Environment from the University of Texas at Austin.
Eric Guenther is an Engineering Scientist at the University of Texas at Austin Center for Space Research where he is a data analyst. He has expertise in machine learning, lidar and GPS analysis. Mr. Guenther holds a B.S. in Geography from Virginia Tech and a Master's degree from Texas A&M University.
Donald Maze-England is an Engineering Scientist Associate at the University of Texas at Austin Center for Space Research where he is a software developer. He has expertise in machine learning, automated feature extraction, software development, and software integration. Mr. Maze-England holds a B.S. in Computer Science from the University of Texas at Austin.
Thomas Bakewell is an undergraduate research assistant at the University of Texas at Austin Center for Space Research. He is working toward a B.A. in Computer Science from the University of Virginia.
Lori Magruder is the Director of the University of Texas at Austin Center for Space Research and an Associate Professor in the Aerospace Engineering and Engineering Mechanics Department. She has expertise with LiDAR experimentation efforts and she has developed many algorithmic approaches for enhanced data exploitation for dedicated scientific and operational applications from other 3D data sources. Dr. Magruder received her B.S. in Aerospace Engineering from the University of Southern California, her Master's degree from Princeton University and her doctorate degree from the University of Texas at Austin.

Computing Predicted Errors and Uncertainty for High Resolution Photogrammetric 3D data

Amy Neuenschwander, Eric Guenther, Donald Maze-England, Thomas Bakewell, and Lori Magruder
Center for Space Research, University of Texas at Austin
3925 W Braker Lane, Austin, TX, 78759
amy@csr.utexas.edu

INTRODUCTION

The utilization of high-resolution 3D point cloud data is becoming more common to a variety of DoD applications and many photogrammetric data sets are collected via small Unmanned Aircraft Systems (sUAS). The quantification of uncertainty in 3D positional data is critically important in many geospatial applications relevant to the DoD. For example, collecting data at an appropriate quality is critical for ISR, targeting, or simulation and training. In simulation and training scenarios a geolocation uncertainty parameter assigned to each model position (e.g. point or vertex) can be integrated into those positions creating an uncertainty ellipsoid about each point. The integration of data uncertainty into a simulation or training environment adds an increased level of realism for the training mission. When considering data collected over a location at two different times, identification of change is always on the forefront of tasks. Incorporating uncertainty estimates is particularly applicable to needs for geospatial model updates with newly acquired data from forward deployed autonomous assets. Although the newest data provides temporally relevant assessments of the terrain, it also could dilute the quality of the overall positioning. It is important to know and subsequently consider data accuracies during any type of data conflation as to track the propagation of errors especially with location-based services and actionable intelligence.

The ability to determine the geolocation accuracy and measurement uncertainty of a sUAS collection is typically done by comparing the input data set against a reference data set or a series of reference known positions. In the case of simulation and training, measurement uncertainty represents the confidence a user can have of the 3D model. Measured errors refer to the errors (bias and uncertainties) obtained via direct comparison of one data set against a reference data set and is implemented as a data validation exercise. As such, measured errors will include registration errors and measurement uncertainties. Registration errors between a high resolution sUAS-photogrammetric input and a reference data can often be represented with an affine transformation that include translations, rotations, and a scale term (ΔX, ΔY, ΔZ, θX, θY, θZ, sf). Registration errors can be computed through the identification of common points in both data sets such as building corners or other permanent targets (Neuenschwander et al., 2023). These registration errors are often expressed as an overall bias (horizontal and vertical) and a root mean square error (horizontal and vertical). In many cases though, an expression of overall bias and RMSE, is not good enough. Errors and uncertainties need to occur on a per-point basis. After the registration step, the residual differences between the registered input point cloud and the reference point cloud represent a per-point measurement uncertainty. In the case of photogrammetric 3D data, this per-point measurement uncertainty pertains to not only an overall geolocation uncertainty but also include issues related to the geometric or structural representation of the data.

A traditional data validation procedure, however, may not always be feasible for all sUAS data collections; particularly if sUAS data are collected for operations and require a quick turn-around. The goal of this research is to generate per-point predicted errors from sUAS-photogrammetric data such that they closely approximate the measurement errors as shown in Figure 1. The ability to quantify the 3D predicted accuracy of a sUAS collect is dependent upon multiple factors including sensor type. For lidar collections where information regarding the quality of the differential GPS (DGPS) and high accuracy inertial measurement unit (IMU) solutions as well as laser calibration parameters are typically available, the geolocation uncertainty can be described through rigorous error modeling as outlined by (Glennie, 2007; Schaer et al., n.d.). For photogrammetrically (EO) derived 3D data, the sUAS platform may not be DGPS capable and positional data is collected using pseudorange GPS. Thus, less information to produce a 3D predicted accuracy is typically available for photogrammetric derived 3D data product. Generally speaking, the quality

of a photogrammetric derived 3D data product is also contingent upon the data acquisition procedure and reconstruction process.

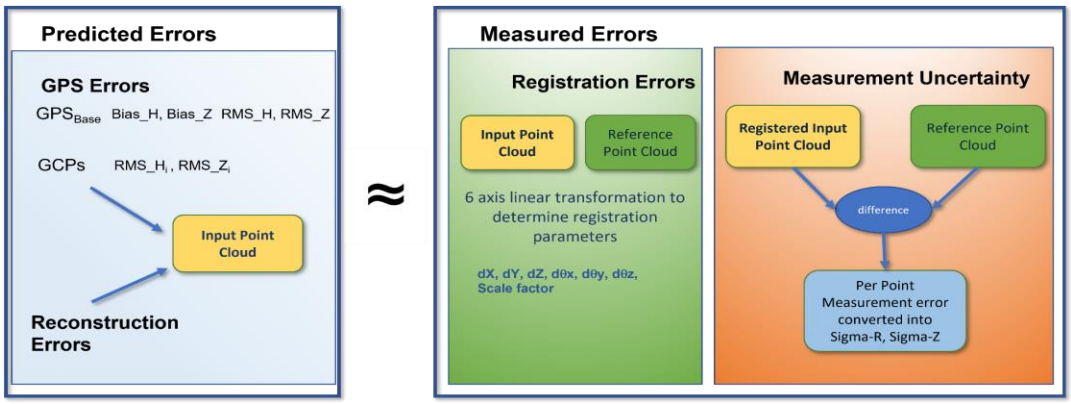

Figure 1. Overview of Error/Uncertainty sources for sUAS-Photogrammetric 3D Data.

When considering the predicted errors of sUAS-photogrammetric point clouds/meshes, the two primary elements of consideration are the errors and uncertainties from the GPS and any structural errors due to the 3D reconstruction process. In many instances, the GPS errors and uncertainty from the sUAS positioning may not be known as most small photogrammetric sUAS platforms do not record that information. Thus, the X,Y,Z position attached to each photograph is obtained with pseudorange GPS. Utilizing the pseudorange GPS positions in the 3D reconstruction process will result in registration or geolocation errors. In these cases, the geolocation errors can only be determined by directly comparing the input data against a known, reference data source. There are, however, instances where the geolocation errors can be mitigated or reduced through the collection of independent field ground control points (GCPs) as part of a calibration/validation effort as the data are being collected. The use of survey-grade GPS in conjunction with the collection of ground control points are an excellent way to independently quantify potential geolocation errors due to poor sUAS GPS. By utilizing best practices when collecting GPS positions on ground control points and subsequently using those GCPs within the 3D reconstruction (Structure for Motion, SfM) software, the geolocation (or registration) errors are significantly minimized.

Structural or reconstruction errors are often present in photogrammetrically derived point clouds and meshes and can be attributed to shadows in the sUAS photos, a lack of contrast on a surface, or not enough photos or "looks" on the target. In the case of buildings, the result is often rounded corners, planar surfaces not planar, and distortions in doorways and windows. An example of a structural error from the 3D Reconstruction process is shown in Figure 2. In this Figure, the per-point error is calculated as the 3D distance between input SfM point cloud and a reference point cloud and large errors are observed in the inside building corner, doorways, and windows.

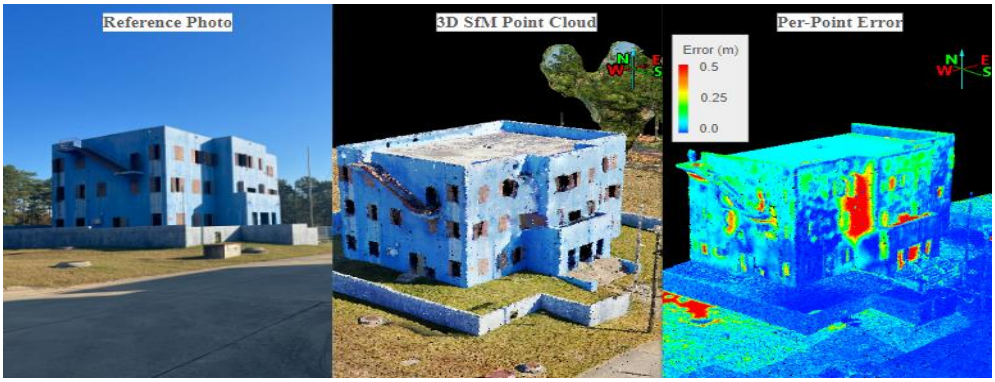

Figure 2. Example of errors introduced during SfM reconstruction. A majority of measurements are accurate to within 5 cm, however, certain areas exhibit high error, including corners, certain topographic features, and around windows and doors. The per-point error was calculated against a high-accuracy terrestrial laser scan.

DATA

Field Site

A 3D high resolution data collection occurred at Ft Moore, Georgia at the Selby Combined Arms Collective Training Facility (CACTF) site on November 11, 2023. The collection included a sUAS-Photogrammetry acquisition as well as a Terrestrial Lidar Scanning (TLS) survey of the building exteriors. In addition, a real-time differential GPS (DGPS) survey of ground control points and other targets was conducted for data calibration and validation.

GPS Data

GPS data were collected using a Trimble R12i receiver and the CenterPoint RTX real-time differential correction subscription available from Trimble. Several independent studies investigating the accuracy of RTX report horizontal and vertical accuracies of 1 and 2.5 cm respectively (Ozer Yigit et al., 2022). In addition to the utilization of the RTX real-time service on the Trimble rover, a Trimble receiver was set up as a static base station operating at a 30 second rate. A RTX position was collected on the base station point at the beginning of the survey as well as at the end of the survey, roughly five hours later. The GPS base station data was processed using the Online Positioning User Service (OPUS) provided by NOAA National Geodetic Survey. GPS base station coordinates are reported in both geographic coordinates (latitude and longitude) as well as UTM projected coordinates with the WGS84-2010/ITRF 2010 ellipsoid to represent the vertical heights. The computed difference between the base station position determined via OPUS and the RTX position was computed to be 0.074 m and -0.013 m, horizontal and vertical respectively with 0.008 and 0.006 m RMS.

Ground Control Points

Several papers in the open literature have explored the relationship between number and distribution of GCPs on the final data accuracy. When flying sUAS collections for high resolution data, the typical size of our Area of Regard (AOR) is approximately 500 x 300 m or 0.15 km^2. When flying low (~50 m or less), our goal is to have a minimum of six GCPs distributed evenly across the AOR. The suggested standard for the number of GCPs is ~40 to 50 per 1 km^2, however, the number and distribution depends upon the topography and the elements within the AOR (Oniga et al., 2018). Thus, for an area the size of 0.15 km2, six to eight GCPs well distributed across the AOR would be the recommendation. In a similar study, the utilization of more than 10 GCPs was found to have little influence on reducing the overall RMSE, however the placement of the GCPs was critical (Oniga et al., 2018). Placement of the GCPs should be distributed across the entire AOR and should avoid straight lines and avoid being clustered in one particular region of the AOR. Furthermore, it is recommended to place some GCPs near the edge of the AOR as these data will likely be conflated with other data sets. Improved accuracy at the edges of the AOR will reduce the impact or presence of seams or elevation discrepancies with other data. The quality of the GCP positions is directly related to the quality of the GPS system that is used to measure the X,Y, Z position of each GCP. For this survey, six GCPs were placed within a 0.15 km2 area. For this collection, the geolocation RMSE (i.e. the uncertainty) of the GCP positions ranged from 0.7 to 0.8 cm, horizontal and 1 to 1.3 cm vertical. The error term associated for each GCP is assumed constant and is the same bias observed between the OPUS position and RTX position for the base station of 0.074 m and -0.013 m, horizontal and vertical. In addition to placement of the ground control points with the AOR, additional validation GPS positions were recorded at easily identifiable locations in the input data such as building corners at ground level and wall points.

sUAS-EO Data

The sUAS data were collected from a Skydio X2D system which is equipped with only a pseudorange code GPS; thus differential correction through either a Real Time Kinematic (RTK) or Post Processing Kinematic (PPK) was not possible. The Skydio X2D is equipped with a 12 M Pixel camera and has obstacle avoidance capabilities that allows for easier piloting at lower altitudes for more detailed collection. The pose information from each Skydio X2D photo includes a position (X,Y, Z) where Z is height above the reference ellipsoid and orientation angles of omega (rotation about the x-axis), phi (rotation about the y-axis) and kappa (rotation about the z-axis). The Context Capture software was used to construct a 3D mesh from the raw photos using Structure from Motion. Within Context Capture, positions from the GCPs were used to warp the 3D mesh from the geolocated positions inferred from the Skydio X2D GPS coordinates into absolute geolocation positions. Next, a point cloud with a 10 cm resolution was then derived from the 3D mesh product. The 3D point cloud is referred to here as the input sUAS-EO point cloud. To illustrate the impact of incorporating GCPs into Context Capture (or any SfM software), a second point cloud was created where the GCPs were not used in the 3D reconstruction process.

Terrestrial Lidar Scanner Data.
TLS data were collected at the Selby CACTF site using a Trimble X7 laser scanner. The Trimble X7 utilizes a self-registration from each scanning position creating high accuracy 3D point clouds. When collecting TLS data of building exteriors, the goal is to obtain multiple views such that occlusions are minimized or eliminated. For this survey, 42 TLS scans were combined to generate a point cloud of over 51 million points and a point density of 1929 pts/m^2. Data from the TLS were placed into absolute geolocation positions (UTM projection, WGS84 Epoch 2010 ellipsoid) using the same GCPs targets as were used to anchor the input sUAS-EO data as well as a few additional targets visible during the TLS scans. By placing the TLS data into absolute real-world coordinates, the TLS data serves as a very high spatial resolution reference data source. For the purposes of this analysis, the TLS data were manually cleaned to remove spurious noise points, birds, wires, and people from the point cloud. The TLS and sUAS-EO input point cloud were then cropped to have the same geographic extent as shown in Figure 3 (yellow box). The positions of the GCPs and the GPS base station are also indicated in Figure 3.

Figure 3. Overview of Selby Collection Site with Ground Control Points marked. The region within the yellow box was used for further analysis.

An example of the structural/reconstruction errors is shown in Figure 4. Here a 0.5 x 27 m profile is pulled across a building within the AOR from both the input sUAS-EO point cloud and TLS data. In this profile, the reconstruction errors along the side of the building as well as the roof extend roughly 75 cm in both the horizontal and vertical directions. The cause of the reconstruction errors is likely due to low contrast and poor correlation between photos. This type of error is observed in the majority of the buildings within the AOR, however, the magnitude of the error can range from 30 cm to over 3 m. Incorporating these reconstruction errors into a predicted error for the data set could have great impact for determining the usability of the collected data for various purposes related to training or targeting.

Figure 4. Profile of a building within the AOR illustrating the structural reconstruction errors.

METHODS

Derivation of per-point predicted error from GPS/Ground Control Points

As described in Figure 1, the predicted uncertainty for Photogrammetrically derived 3D data should be comprised of both GPS errors and structural/geometric errors from the 3D reconstruction process. To establish a per-point-uncertainty due to GPS, the horizontal and vertical uncertainties from the six GCP positions were interpolated across the entire point cloud (Figure5 and 6, respectively) using an inverse distance weighting method. The uncertainties when using the CenterPoint RTX were observed to be less than 1 cm in both the horizontal and vertical direction. The uncertainty values of 0.008 and 0.006 m, horizontal and vertical respectively from the OPUS solution for the GPS base station were added to the per-point values of the GCP propagated uncertainty values.

Derivation of per-point Measurement Error and Uncertainty

As both the TLS reference data and the input sUAS-EO point cloud used the same GCPs to anchor into absolute real-world coordinates, it is assumed that there are no registration errors between the two data sets. In an absolute space, however, there is a bias and uncertainty value based upon the accuracy of the RTX GPS positions and those errors will factor into the overall error budget for this particular AOR. The objective, however, of this research is to explore the feasibility of generating a model to estimate the per-point predicted error that approximates the actual 3D measured error. To calculate this measurement uncertainty, the 3D distance between the closest point for the input sUAS-EO data and the TLS data set was computed. Figure 5 illustrates the 3D distance error where the 3D errors range between 0 and 0.5 m limited by the search radius of 0.5 m. Many of the building roofs show an error of 0.5 m, however, there were no roofs in the TLS data for these buildings; thus the errors shown on the roof are a false error. Most of the true observed error corresponds to doorways and windows on the buildings.

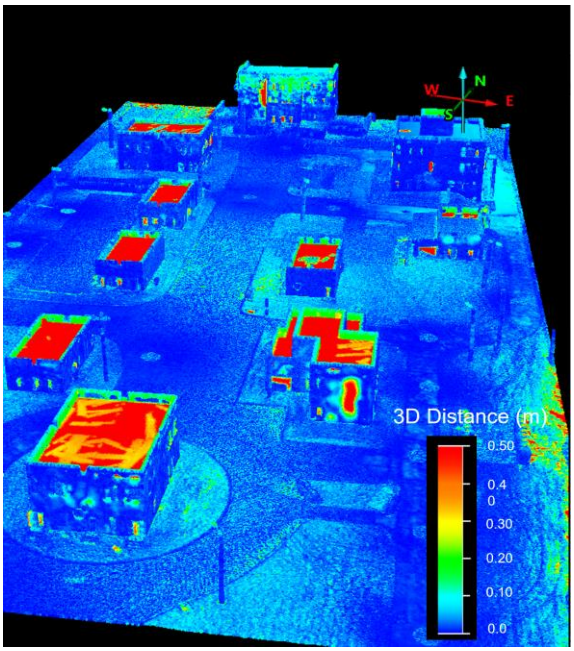

Figure 5. 3D Distance between the input and reference data representing the Measurement Uncertainty.

Deriving a Model to Predict Measurement Uncertainty

As illustrated in Figure 5, structural errors from the reconstruction process are likely the largest contributor of error/uncertainty as the GPS uncertainties are relatively small because GCPs were used to reduce registration errors. To successfully implement a model to predict the measurement error, the model inputs must be derived directly from the sUAS-EO input point cloud. For this research, a comprehensive exploration of Feature Engineering was executed to identify the most predictive features that can be derived from the data for estimating errors and uncertainties. First, a series of normal vectors based on the first principal component with a defined radius ranging from 10 cm to 1 m

(increments of 10 cm) was computed. A normal vector having a value of 0 indicates a vertical wall whereas a value of 90 indicates a horizontal surface (i.e. roof or terrain). Normal vectors calculated with a 20 cm (Figure 6 left panel) and 50 cm radius (Figure 6 right panel) both reveal discrepancies from a planar, vertical surface as normal vectors greater than 88 degrees are not plotted. The regions of large normal vectors, that is with values greater than 3 degrees and less than 55 degrees, often occur in doorways, windows, and rooftop edges. In addition to the normal vectors, a height change (dH) using a mean shift algorithm, an omnivariance calculated at 0.2 m, and an anisotropy metric also calculated at 0.2 m were used as input features into the model.

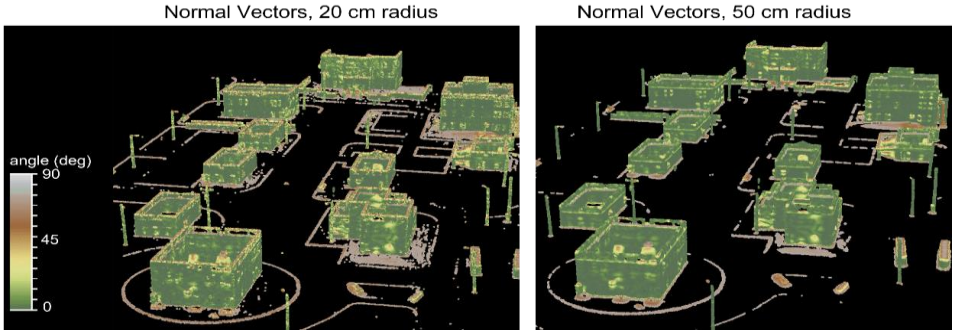

Figure 6. Normal vectors calculated on the input point cloud (UAS-EO) using a 20 cm (left panel) and 50 cm (right panel) radius. The normal vectors are plotted from 0 to 88 degrees.

For this analysis, a machine learning gradient boosted regression (GBR) was the model architecture tested. A GBR algorithm is similar to a Random Forest in that decision trees are used to make predictions, however, with a GBR the decision trees are built sequentially. Under this construct, each GBR decision tree focuses on correcting errors from the previous trees by fitting to the residual errors of the previous fit. The benefit of using this model is by fitting the decision trees to prior error, the overall accuracy of the model improves. Each model was trained on the normal vectors at 20 cm, 50 cm, and 1 m along with the DH component, omnivariance, and anisotropy with the 3D measurement uncertainty data serving as the reference. Over time as more data are collected, the uncertainty model will likely improve.

RESULTS AND DISCUSSION

GPS/Ground Control Points Results

For this research, we tested the importance of using GCPs during the photogrammetric reconstruction process. Additional validation points were used to calculate the registration errors for the sUAS input point cloud that were created with and without GCPs. The registration errors listed in Table 1 show that without using GCPs, the overall errors were 0.98 m and -8.65 m in the horizontal and vertical directions. When GCPs were incorporated during the reconstruction process, those geolocation errors were reduced to 5.9 cm horizontal and -7.5 cm vertical. Another benefit of using GCPs is not only that the 3D model is placed into the correct geodetic space, but localized distortions (potentially from the camera lens) are reduced subsequently resulting in a more accurate relative and absolute 3D model. In terms of absolute geolocation errors for this AOR, the registration errors listed in Table 1 would be added to the geolocation offset of the GPS base-station location which was computed to be 0.133 m (0.059 m + 0.074 m) and -0.088 m (-0.013 + -0.075 m), horizontal and vertical respectively.

Table 1. The computed mean and standard deviation registration errors in meters for EO-point cloud data within the AOR

	dX	dY	dH	dZ
3D Data without GCPs	-0.356 (0.398)	-0.794 (0.253)	0.980 (0.139)	-8.656 (0.863)
3D Data with GCPs	-0.006 (0.045)	0.023 (0.064)	0.059 (0.056)	-0.075 (0.058)

The impact of incorporating GCPs into the 3D reconstruction is evident by the reduction in overall horizontal and vertical error. The computed statistics, however, do not tell the whole story. The utilization of GCPs within the 3D reconstruction constrains the fit and minimizes distortions and warping that may otherwise occur due to camera lens

distortions. To illustrate this effect, the 3D distance error was calculated between the two sUAS point clouds; with and without GCPs and the result is presented in Figure 7. For this particular collection, in addition to the ~8.6 m vertical and 1 m horizontal difference, there are localized non-linear variations up to 3 m on the terrain points between the two data sets illustrating the importance of GCPs when collecting sUAS data.

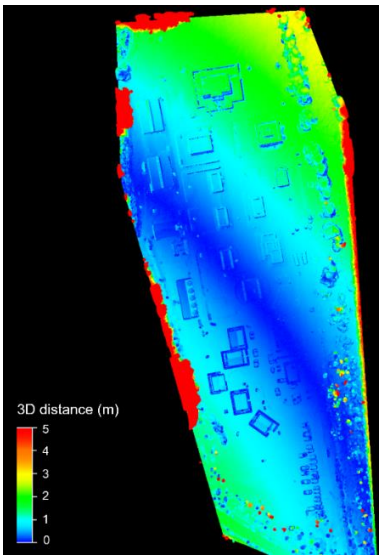

Figure 7. 3D error distance calculated between two sUAS point cloud data sets where GCPs were and were not used in the 3D reconstruction.

Per-Point Error Estimation Model Results

The results for GBR estimated measurement uncertainty are illustrated in Figure 8. While not perfect, the GBR model does place higher uncertainties in locations where the uncertainties exist in the reference data. Namely, many windows, doorways, and beneath covered patios were predicted to have the largest uncertainties. As more data become available with both the sUAS-EO model and TLS as reference, the GBR model (or potentially another model architecture) can be updated to be more representative. These predicted measurement uncertainty values would be combined (added) to the GPS uncertainty values to create an overall predicted per-point uncertainty. Combined with any known GPS biases, this predicted error establishes a quality metric that can be immediately integrated into the NGA GPM construct and provide an improved characterization of the data quality when external reference data are not available.

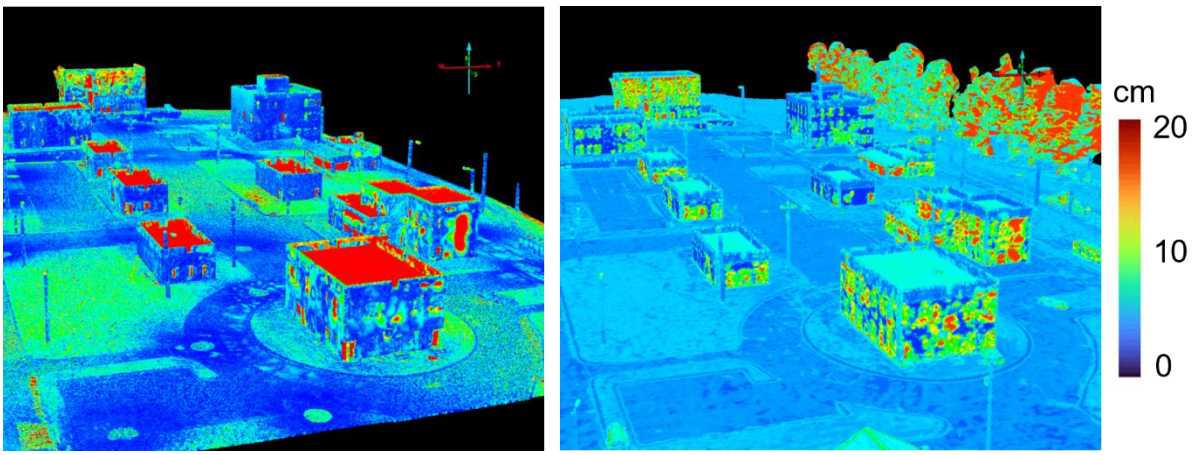

Figure 8. (Left) Reference measurement error calculated as the difference between the TLS data and the sUAS-EO input point cloud (Right) Gradient Boosted Regression Model applied to the entire AOR.

Potential errors not captured (DTM and vegetation errors)

The representation of predicted errors from the error model illustrated in Figure 8 are valid for unobstructed terrain and buildings. The representation of vegetation from photogrammetric data has not yet been tested and assessed. The derived top surface of the canopy would potentially have measurement errors on par with what is represented for buildings. However, the interior structure of vegetation from the ground up is typically not represented since they are not captured in the photographs. For the same reason, the terrain beneath vegetation is often problematic in sUAS-EO 3D data due to lack of penetration. As more data are collected, the GBR model will be updated to improve the representation of other building/object types in the model.

Another type of error that would not be captured as a predicted error are omissions or large holes in walls due to the reconstruction software as shown in Figure 9. Again, likely attributed to poor contrast on the surface, these points are not rendered into a 3D model. Future variants of this research might investigate the fitting of planes to detect these anomalies and incorporate the omissions into the predicted uncertainty. This task, however, is difficult as it would require delineating windows from the omission. A different approach could utilize the detection of windows at the photograph level and pushing those segmentation results to a 3D model. While technically possible, that task is outside of the scope of this current effort.

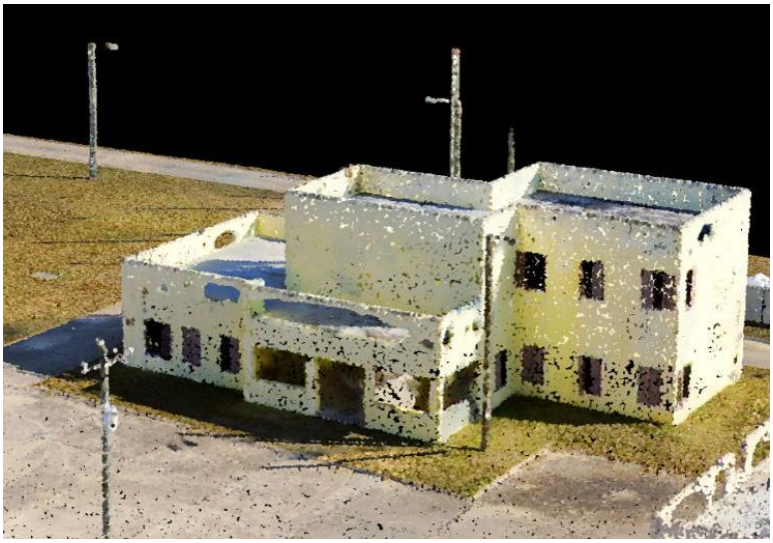

Figure 9. Holes in the parapet walls illustrate reconstruction errors in SfM software.

A key concept for implementing a predicted per-point error estimate on a sUAS collection is the utilization of best practices when collecting the data including the use of ground control targets and a high-quality GPS receiver. In particular, the use of a survey grade differential GPS unit and ground control provides a means to provide the "registration error" component of the diagram in Figure 1. Furthermore, quantification of the GPS errors and uncertainties of the control can be integrated into the predicted errors and uncertainties of the sUAS data. Although the GPS errors and uncertainties are small when collected in the manner described in this paper, they do provide critical knowledge about the overall geolocation accuracy of the data product. Also critical, is the incorporation of the GCPs in the 3D reconstruction process as their usage creates a more accurate relative and absolute data product. Without GCPs, the process for creating a per-point predicted error for photogrammetric 3D data becomes unachievable. The measurement error model developed in this research makes the assumption that there is no registration error (or other warping issues) due to GPS or overall 3D reconstruction.

CONCLUSIONS

High-resolution 3D point cloud data is becoming increasingly important for a variety of DoD applications and continues to gain momentum in reaching geospatial intelligence objectives and operational capabilities. This work addresses a critical challenge when collecting sUAS-derived point cloud data by developing a methodology to predict per-point geolocation uncertainties without the need for extensive validation. Specifically, a model has been developed to predict the geolocation uncertainty when reference data are not available to conduct an independent data validation. This work examines errors on uSAS point clouds when pseudorange code GPS, a commonly used but less accurate

method and differential GPS (DGPS), which provides higher accuracy geolocations, are used to create the data. This study also demonstrated the importance of using ground control points when generating a 3D model. For the data used in this study, overall discrepancies of >8 m vertical were noted however localized relative differences of up to 3m were observed when ground control was not used. Also, a model was developed to predict pre-point errors introduced by the SfM process. By establishing a relationship between these error sources and derived point cloud structural quality, this research provides a pathway to estimate geolocation uncertainties of sUAS data when best practices of data collection are applied. The ability to predict geolocation uncertainties at a per-point level enhances the usability and reliability of sUAS-derived 3D data for DoD simulation and training as well as operational applications.

ACKNOWLEDGEMENTS

This work is sponsored by the U.S. Army Simulation and Training Technology Center (STTC). Many thanks are given to the STTC team of Mr. Clayton Burford, Mr. Gage Jenners, and Ms. Shahira Castellano. Additional thanks are provided to Leidos Corporation: Mr. Tu Lam, Mr. Farid Mamaghani, Mr. Scot Shifflet, and Ms. Amanda Larrieu. Additional thanks are also given to our bird dog, Mr. Corey Hendricks of Leidos Corporation for his guidance and suggestions.

REFERENCES

Glennie, C., 2007. Rigorous 3D error analysis of kinematic scanning LIDAR systems. J. Appl. Geod. 1. https://doi.org/10.1515/jag.2007.017

Lague, D., Brodu, N., Leroux, J., 2013. Accurate 3D comparison of complex topography with terrestrial laser scanner: Application to the Rangitikei canyon (N-Z). ISPRS J. Photogramm. Remote Sens. 82, 10–26. https://doi.org/10.1016/j.isprsjprs.2013.04.009

Neuenschwander, A., Perry, J., and Magruder, 2023. Automated Building Corner Identification for High Resolution 3D Data. Proceedings to the I/ITSEC 2023 Conference, Orlando, Fl. 2023.

Okyay, U., Telling, J., Glennie, C.L., Dietrich, W.E., 2019. Airborne lidar change detection: An overview of Earth sciences applications. Earth-Sci. Rev. 198, 102929. https://doi.org/10.1016/j.earscirev.2019.102929

Ozer Yigit, C., Bezcioglu, M., Ilci, V., Murat Ozulu, I., Metin Alkan, R., Anil Dindar, A., Karadeniz, B., 2022. Assessment of Real-Time PPP with Trimble RTX correction service for real-time dynamic displacement monitoring based on high-rate GNSS observations. Measurement 201, 111704. https://doi.org/10.1016/j.measurement.2022.111704

Schaer, P., Skaloud, J., Landtwing, S., Legat, K., n.d. Accuracy Estimation for Laser Point Cloud Including Scanning Geometry.